

**This is an electronic reprint of the original article.  
This reprint *may differ* from the original in pagination and typographic detail.**

**Author(s):** Kurpeta, Jan; Urban, W.; Płochocki, A.; Rissanen, Juho; Pinston, J.A.; Elomaa, Viki-Veikko; Eronen, Tommi; Hakala, Jani; Jokinen, Ari; Kankainen, Anu; Moore, Iain; Penttilä, Heikki; Saastamoinen, Antti; Weber, Christine; Äystö, Juha

**Title:** Low-spin excitations in the  $^{109}\text{Tc}$  nucleus

**Year:** 2012

**Version:**

**Please cite the original version:**

Kurpeta, J., Urban, W., Płochocki, A., Rissanen, J., Pinston, J.A., Elomaa, V.-V., Eronen, T., Hakala, J., Jokinen, A., Kankainen, A., Moore, I., Penttilä, H., Saastamoinen, A., Weber, C., & Äystö, J. (2012). Low-spin excitations in the  $^{109}\text{Tc}$  nucleus. *Physical Review C*, 86(4), Article 044306. <https://doi.org/10.1103/PhysRevC.86.044306>

All material supplied via JYX is protected by copyright and other intellectual property rights, and duplication or sale of all or part of any of the repository collections is not permitted, except that material may be duplicated by you for your research use or educational purposes in electronic or print form. You must obtain permission for any other use. Electronic or print copies may not be offered, whether for sale or otherwise to anyone who is not an authorised user.

## Low-spin excitations in the $^{109}\text{Tc}$ nucleus

J. Kurpeta,<sup>1</sup> W. Urban,<sup>1,2</sup> A. Płochocki,<sup>1</sup> J. Rissanen,<sup>3,\*</sup> J. A. Pinston,<sup>4</sup> V.-V. Elomaa,<sup>3,†</sup> T. Eronen,<sup>3,‡</sup> J. Hakala,<sup>3</sup> A. Jokinen,<sup>3</sup> A. Kankainen,<sup>3</sup> I. D. Moore,<sup>3</sup> H. Penttilä,<sup>3</sup> A. Saastamoinen,<sup>3,§</sup> C. Weber,<sup>3,||</sup> and J. Äystö<sup>3,¶</sup>

<sup>1</sup>*Faculty of Physics, University of Warsaw, ul. Hoża 69, PL-00-681 Warsaw, Poland*

<sup>2</sup>*Institut Laue-Langevin, 6 rue J. Horowitz, F-38042 Grenoble, France*

<sup>3</sup>*Department of Physics, University of Jyväskylä, P.O. Box 35, FI-40014 Jyväskylä, Finland*

<sup>4</sup>*LPSC, Université Joseph Fourier Grenoble 1, CNRS/IN2P3, Institut National Polytechnique de Grenoble, F-38026 Grenoble Cedex, France*

(Received 29 August 2012; published 2 October 2012)

Monoisotopic samples of  $^{109}\text{Mo}$  nuclei, produced in the deuteron-induced fission of  $^{238}\text{U}$  and separated using the IGISOL mass separator coupled to a Penning trap, were used to perform  $\beta$ - and  $\gamma$ -coincidence spectroscopy of  $^{109}\text{Tc}$ . Spin and parity  $5/2^+$  for the ground state of  $^{109}\text{Mo}$ , proposed earlier, are supported in the present work. Three new low-energy levels observed in  $^{109}\text{Tc}$  are interpreted as bandheads of the  $\pi 3/2^- [301]$ ,  $\pi 5/2^- [303]$ , and  $\pi 1/2^+ [431]$  configurations, respectively. A further three levels observed around 0.4 MeV are interpreted as  $K = 1/2$  triaxial excitations. A similar interpretation is proposed for an analogous set of three levels observed in  $^{107}\text{Tc}$  in another  $\beta^-$  decay work. The systematics of these excitations breaks down in  $^{111}\text{Tc}$ , most likely due to a transition from prolate to oblate deformation. An excitation at 745.0 keV in  $^{109}\text{Tc}$  and 850.7 keV in  $^{107}\text{Tc}$  is interpreted as the  $\pi 7/2^+ [413]$  configuration. Quasiparticle-rotor model calculations support the proposed interpretations.

DOI: [10.1103/PhysRevC.86.044306](https://doi.org/10.1103/PhysRevC.86.044306)

PACS number(s): 23.20.Lv, 23.40.-s, 25.85.Ge, 27.60.+j

### I. INTRODUCTION

The neutron-rich  $^{108}\text{Ru}$  nucleus has been predicted to have the highest energy gain due to triaxial deformation throughout the nuclear chart [1]. One may thus expect a variety of phenomena associated with triaxiality in nuclei around  $^{108}\text{Ru}$ . An example is a transition from  $\gamma$ -soft vibrations in neutron-rich Mo isotopes, where, in  $^{106}\text{Mo}$ , one finds the best known example of a double-phonon  $\gamma$ -vibrational state [2], toward triaxial rotors in neutron-rich Ru isotopes [3]. Another interesting effect expected in this region is the transition from triaxial-prolate deformation toward an oblate deformation [4–6]. Our recent study of excited states in  $^{111}\text{Tc}$  populated in the  $\beta^-$  decay of  $^{111}\text{Mo}$  has provided the first clear signature in favor of an oblate deformation in  $^{111}\text{Tc}$  [7], which makes the  $A \sim 110$  region the second location on the nuclear chart where this rare phenomenon is observed. The key nuclei in which these transitions should be manifested are the neutron-rich isotopes of Tc.

The evidence for an oblate shape in  $^{111}\text{Tc}$  is based on the observation of low-energy configurations, which are not expected in the prolate minimum of the nuclear potential, while

they appear in the oblate minimum. In  $^{111}\text{Tc}$  the candidate for an oblate configuration is the  $5/2_2^+$  level at 42.6 keV, located just above the  $5/2^+$  ground state dominated by the  $5/2^+ [422]$  prolate configuration. There is thus a coexistence of prolate and oblate excitations in  $^{111}\text{Tc}$ . Furthermore, as indicated in a more advanced theoretical study of nuclei in this region [8,9], one may also observe a mixing between the prolate and oblate solutions. A simple calculation within the Nilsson scheme applied in our work to  $^{111}\text{Tc}$  [7] was able to account for both the prolate and oblate  $5/2^+$  levels mentioned above, but it was not able to explain a new  $3/2^+$  level at 30.7 keV. It is possible that this level results from mixing of both types of deformation. It is of interest to find arguments which could help to verify these suggestions.

The systematic observation of various nucleon configurations along isotopic or isotonic lines can be very helpful in these respect. Several recent studies of odd- $A$ , neutron-rich Tc isotopes [6,10–16] have established basic proton configurations in these nuclei. Up to  $^{107}\text{Tc}$ , having  $N = 64$  neutrons, these configurations are well known and vary smoothly with the neutron number, as can be seen in Fig. 1(a). These are the prolate proton configurations  $3/2^- [301]$ ,  $5/2^- [303]$ , and  $5/2^+ [422]$ . The  $\pi 5/2^+ [422]$  configuration is observed also in  $^{109}\text{Tc}$  and  $^{111}\text{Tc}$ , but the  $\pi 3/2^- [301]$  and  $\pi 5/2^- [303]$  levels are not known in these two nuclei.

Figure 1(a), which shows prolate configurations, does not indicate any second  $5/2^+$  level at low energy in  $^{111}\text{Tc}$ . Therefore the  $5/2_2^+$  level at 42.6 keV in  $^{111}\text{Tc}$  is a good candidate for an oblate configuration. However, for the low-lying  $3/2^+$  level seen at 30.7 keV in  $^{111}\text{Tc}$ , the situation is not so obvious. In Fig. 1(b) we show energies of  $3/2^+$  members of the  $\pi 1/2^+ [431]$  intruder band. (The  $\pi 1/2^+ [431]$  level is, in most cases, located above the  $3/2^+ [431]$  level, due to large decoupling.) The  $1/2^+ [431]$  intruder band is firmly identified in a number of Ag and Rh odd- $A$  isotopes and in  $^{105,107}\text{Tc}$  (and there is also a likely candidate in  $^{103}\text{Tc}$ ). If the variation

\*Present address: Nuclear Science Division, Lawrence Berkeley National Laboratory, Berkeley, California 94720, USA.

†Present address: Turku PET Centre, University of Turku, FI-20521 Turku, Finland.

‡Present address: Max-Planck-Institut für Kernphysik, Saupfercheckweg 1, D-69117 Heidelberg, Germany.

§Present address: Cyclotron Institute, Texas A&M University, College Station, Texas 77843-3366, USA.

||Present address: Fakultät für Physik, Ludwig-Maximilians-Universität München, Am Coulombwall 1, D-85748 Garching, Germany.

¶Present address: Helsinki Institute of Physics, P.O. Box 64, FI-00014 University of Helsinki, Finland.

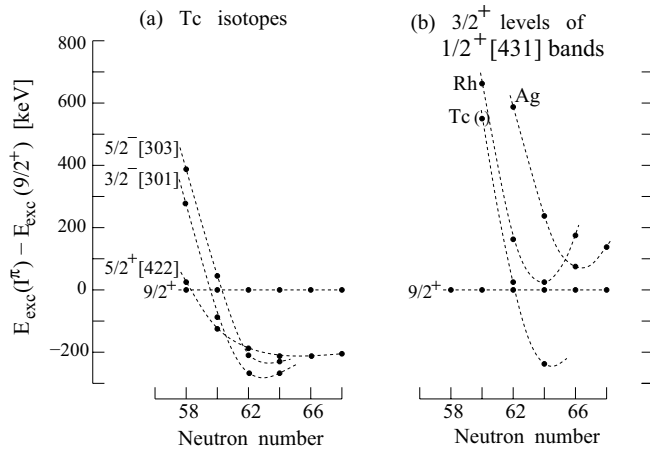


FIG. 1. Systematics of proton configurations in neutron-rich Tc isotopes and  $3/2^+$  levels in Tc, Rh, and Ag, drawn relative to the  $9/2^+$  member of the  $\pi 5/2^+[422]$  configuration. The data are taken from Refs. [6,10–12]. The dashed lines are drawn to guide the eye.

of the  $3/2^+$  excitation energy in the Tc isotopes is similar to that observed in the Ag and Rh isotopes, then one may expect in  $^{109}\text{Tc}$  a  $3/2^+$  level close to the  $5/2^+[422]$  ground state. Furthermore, the  $3/2^+$  member of the  $\pi 1/2^+[431]$  intruder band should be located well above the  $\pi 5/2^+[422]$  ground state in  $^{111}\text{Tc}$ . Consequently, the  $3/2^+$  level at 30.7 keV in  $^{111}\text{Tc}$  may be due to an oblate (or a mixed prolate-oblate) configuration.

It is then clear that searching for further proton configurations in  $^{109}\text{Tc}$  and extending the systematics shown in Fig. 1 is vital for further studies of oblate deformation in the mass  $A \sim 110$  region. This became the main motivation of the present work, dedicated specifically to searching for new low-energy bandheads in  $^{109}\text{Tc}$ . We note that, apart from looking for the  $\pi 1/2^+[431]$  intruder band, it is equally important to search for the  $\pi 3/2^-[301]$  and  $\pi 5/2^-[303]$  configurations, which are expected near the  $\pi 5/2^+[422]$  level in  $^{109}\text{Tc}$ . In our previous study of  $^{109}\text{Tc}$  [13] we have identified a band which may correspond to one of these configurations and found an upper limit for the energy of its bandhead. The observation of this bandhead would support the use of the excitation-energy systematics.

Furthermore, as pointed out in Ref. [13], there may be nonyrast excitations in  $^{109}\text{Tc}$  corresponding to  $\gamma$  vibrations coupled to the  $5/2^+[422]$  ground state. The yrast members of  $\gamma$  bands, with spins 9/2 or higher, were observed in measurements of prompt  $\gamma$  rays from fission [13]. It would be interesting to check whether these low-spin excitations are related to low-spin levels in  $^{111}\text{Tc}$ , such as the 30.7-keV level.

This article is presented as follows: in Sec. II we describe our experiments; in Sec. III we present the experimental results, which are then discussed in Sec. IV. The work is summarized in Sec. V.

## II. EXPERIMENTS

The  $^{109}\text{Mo}$  nucleus has been investigated in two independent experiments carried out at the Ion Guide Isotope Separator On-Line (IGISOL) facility [17] of the University of Jyväskylä.

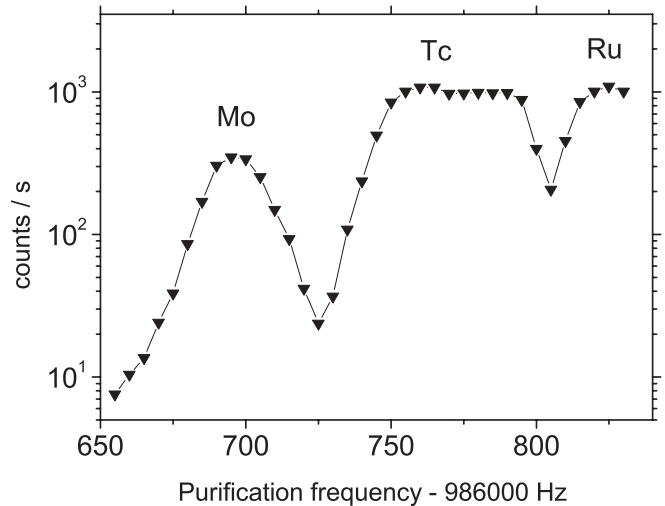


FIG. 2. Ion counts registered in the second experiment using an MCP detector placed after the Penning trap. The resolved atomic ions from the IGISOL isobaric beam of  $A = 109$  are marked with their element symbol. Note that the Tc count rate is highly saturated.

In both experiments  $^{109}\text{Mo}$  nuclei were produced in fission induced by 25-MeV deuterons irradiating a natural uranium target. Fission products were on-line mass separated with the IGISOL3 [18] mass separator. The isobaric beam of ions from IGISOL3 was directed into a radio-frequency cooler-buncher [19] from where ions were sent to the purification Penning trap of the JYFLTRAP setup [20–22], where isobaric contaminants were removed using buffer gas cooling technique [23]. Figure 2 shows the spectrum of ions with mass  $A = 109$ , measured after the Penning trap using a micro channel plate (MCP) detector. The measurement was done by scanning the quadrupole electric field frequency over the cyclotron frequency  $f = \frac{1}{2\pi} \frac{q}{m} B$ , where  $q$  and  $m$  are the charge and mass of the ion and  $B$  is the magnetic field inside the trap. Transmission of ions occurs only near the cyclotron frequency of the ions. As seen in Fig. 2, JYFLTRAP can deliver a monoisotopic beam of  $^{109}\text{Mo}$  with a mass resolving power  $M/\Delta M_{\text{FWHM}}$  of about 40,000.

The  $^{109}\text{Mo}$  ions, released from the trap, were implanted into a plastic tape used to remove the long-lived decay products at regular intervals. Our detector setup consisted of a 2-mm-thick plastic scintillator surrounding the implantation point, used for detecting electrons from  $\beta$  decay, two 120% Ge detectors for measuring  $\gamma$  rays, and a low-energy photon spectrometer (LEPS) used to measure low-energy  $\gamma$  rays. In the first experiment the data acquisition system was triggered when a signal from the  $\beta$  scintillator was in time coincidence with a signal from any of the  $\gamma$  detectors. In the second measurement the data acquisition was triggered by a signal from any of the  $\gamma$  detectors or the  $\beta$  counter.

In the first experiment a fresh sample of  $^{109}\text{Mo}$  ions was implanted into the collection tape every 111 ms. The tape was moved every 300 s to remove the excessive activity. Due to the long time interval between tape movements one can observe a high intensity of  $\gamma$  transitions associated with the long-lived isobars of the  $^{109}\text{Mo}$  decay chain, as shown in Fig. 3. In the second run a fresh ion sample was delivered every

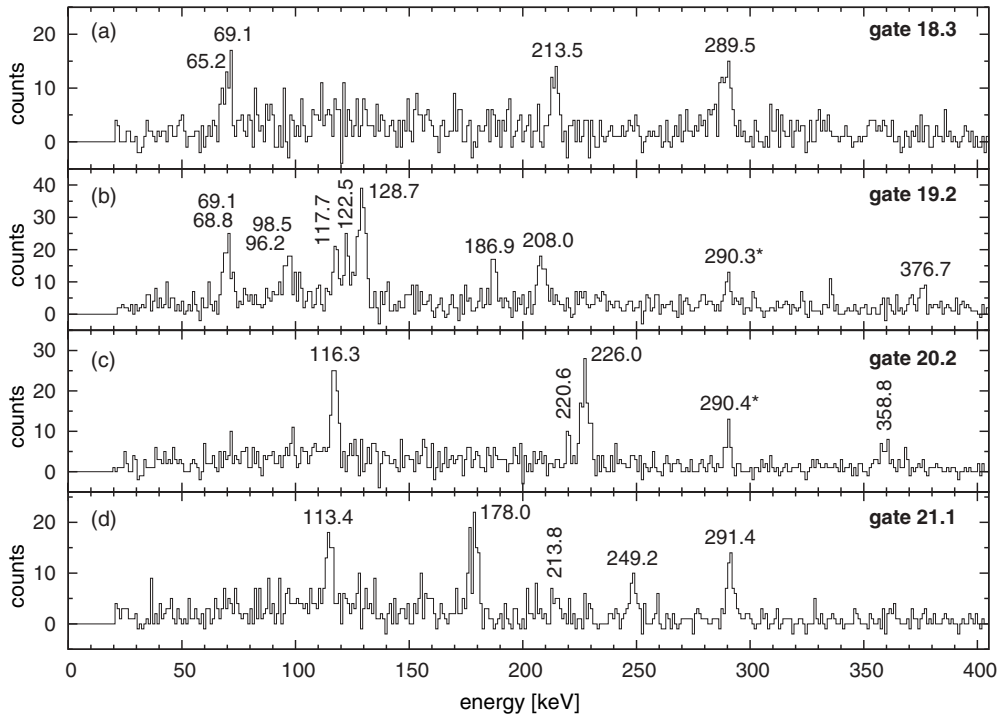


FIG. 3. The sum of spectra measured in the two Ge detectors in coincidence with  $K_\alpha$  x rays of (a) Tc, (b) Ru, (c) Rh, and (d) Pd in the LEPS detector. The collection tape was moved every 300 s. The peaks marked with an asterisk result from partial overlap of Tc and Ru  $K_\alpha$  x rays (b) and overlap of Tc  $K_\beta$  and Rh  $K_\alpha$  x rays (c). Peak and gate energies are given in keV.

121 ms and the collection tape was moved after 9 subsequent implantations. Therefore the activity due to long-lived isobars was considerably reduced. In the first measurement the rate of  $^{109}\text{Mo}$  ions counted with the MCP was about 430 counts/s and in the second run it was about 560 counts/s.

### III. RESULTS

The  $\beta^-$  decay of  $^{109}\text{Mo}$  was studied earlier with the IGISOL mass separator without the Penning trap setup [24,25]. A half-life of 0.53(6) s was obtained and two  $\gamma$  lines at 65.1 and 289.1 keV were assigned based on coincidence with Tc  $K$  x rays.

#### A. Identification of elements

In the measurement in which the long-lived daughters of  $^{109}\text{Mo}$  were observed it was possible to distinguish  $\gamma$  lines belonging to a given element by gating on a respective  $K_\alpha$  x-ray peak in the LEPS detector. Our data shown in Fig. 3(a) confirm the coincidence between Tc  $K_\alpha$  x rays and the  $\gamma$  lines at 65 and 289 keV. The spectrum in Fig. 3(b) was gated on Ru  $K_\alpha$  x rays and shows  $\gamma$  lines in  $^{109}\text{Ru}$  fed by the  $\beta$  decay of  $^{109}\text{Tc}$ . Similarly, the spectra in Figs 3(c) and 3(d) were gated by Rh and Pd  $K_\alpha$  x rays and they show  $\gamma$  lines fed by the  $\beta$  decay of  $^{109}\text{Ru}$  and  $^{109}\text{Rh}$ , respectively.

#### B. Beta decay scheme of $^{109}\text{Mo}$

The scheme of excited levels in  $^{109}\text{Tc}$  was constructed based on  $\gamma\gamma$  coincidence relations between  $\gamma$  rays following the  $\beta$

decay of  $^{109}\text{Mo}$ . Coincidence  $\gamma$  spectra measured with Ge detectors, gated on  $K$  x-ray lines seen in the LEPS detector, enabled the discovery of new lines populated in the  $^{109}\text{Mo}$  decay [Fig. 3(a)] and helped us to identify  $\gamma$  lines from the less exotic nuclei in the  $\beta$  decay chain. Examples of coincidence  $\gamma$  spectra from the LEPS detector, gated by  $\gamma$  lines in the Ge detectors, are shown in Fig. 4. Such spectra allowed coincidence relations to be made between low-energy  $\gamma$  lines and, in some cases, to estimate their internal conversion coefficients. The resulting scheme of excitations populated by the  $^{109}\text{Mo}$   $\beta^-$  decay is shown in Fig. 5. The intensities and coincidence relations of  $\gamma$  lines in  $^{109}\text{Tc}$ , as observed in this work, are listed in Table I.

We confirm the 69.1- and 137.0-keV transitions reported in the yrast cascade of  $^{109}\text{Tc}$  in the prompt- $\gamma$  measurement of  $^{248}\text{Cm}$  spontaneous fission fragments [13]. Several new  $\gamma$  lines are observed in the  $\beta$  decay of  $^{109}\text{Mo}$  as compared to the prompt- $\gamma$  measurement [13]. Their coincidence relations allowed new, low-energy excited states in  $^{109}\text{Tc}$  to be established at 7.0, 18.0, 50.4, 333.1, 358.6, 423.8, and 489.0 keV, as shown in Fig. 5.

Comparing the spectra in Figs. 3(a) and 3(b) one can see the line at 69.1 keV present in the  $\beta$  decay of both  $^{109}\text{Mo}$  and  $^{109}\text{Tc}$ . In the decay of  $^{109}\text{Tc}$ , there is a  $\gamma$  line with a very similar energy of 68.8 keV with an intensity even higher than that of the 69.1-keV line. Moreover, in the  $\beta$  decay of  $^{109}\text{Ru}$  there is a 68.1-keV line, which partially overlaps with the 69.1-keV line. Even the data recorded in a run when the collection tape moved every second do not discriminate between the intensities fed by  $^{109}\text{Mo}$  and  $^{109}\text{Tc}$  decays as their half-lives of 0.53 and

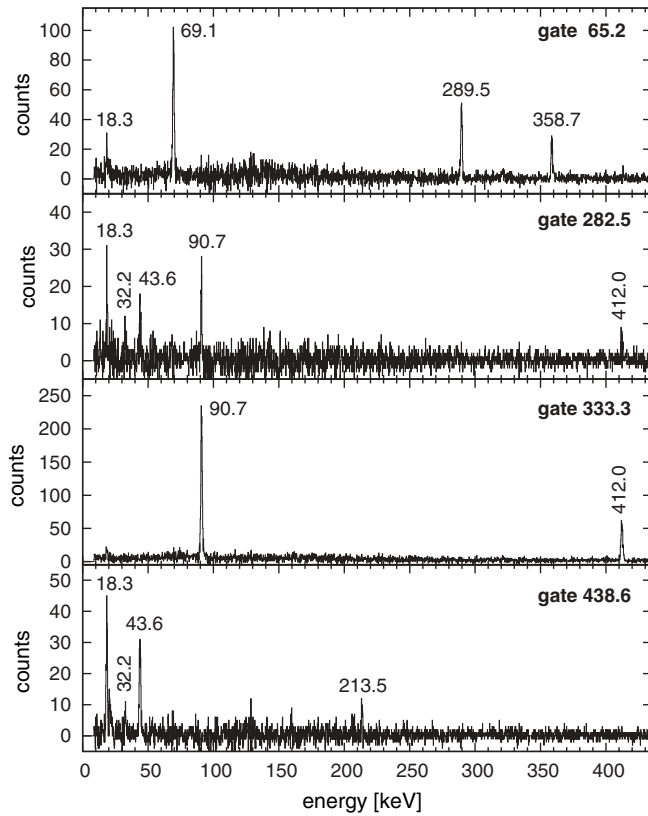


FIG. 4. Coincidence  $\gamma$  spectra in the LEPS detector gated by peaks in two 120% Ge detectors in the second run. Peak and gate energies are given in keV.

0.86 s are too similar. Consequently, it is difficult to estimate the true intensity of the 69.1-keV transition populated in the  $\beta^-$  decay of  $^{109}\text{Mo}$  by simple subtraction of the components coming from the transitions in the daughter isobars. By using a coincidence spectrum gated by the 65.2-keV line, the intensity of the 69.1-keV transition was estimated to be higher than  $53 \pm 17$ . By subtracting components of the 69.1-keV transition coming from the 69.1- and 68.8-keV lines in  $^{109}\text{Ru}$  and from the 68.1-keV transition in  $^{109}\text{Rh}$ , one can roughly estimate the intensity of the 69.1-keV line belonging to the  $\beta$  decay of  $^{109}\text{Mo}$  as  $44 \pm 15$ . In summary, the  $\gamma$  intensity of the 69.1-keV line fed by the  $\beta$  decay of  $^{109}\text{Mo}$  can be estimated to be higher than or equal to 19 and not larger than 74, if one assumes an uncertainty of two standard deviations (see Table I). By taking into account the balance of transitions populating and decaying out of the 69.1-keV level, its maximum  $\beta$  feeding can be estimated to be  $3 \pm 1$ , which sets a lower limit of 6.3 for  $\log ft$ , as shown in Table II.

The short (1 s) and long (300 s) collection-tape cycles in our two measurements provide a hint on the origin of  $\gamma$  lines, based on their half-lives, because the ratio of  $\gamma$  intensities seen in the two measurements (see Fig. 6) depends on the  $\beta$  decay half-life. In this way we assigned the 165.0-keV line to the decay of  $^{109}\text{Mo}$ , while this line is observed in singles spectra, only, and does not show any coincidence relations. A  $\gamma$  line of the same energy was reported in a prompt- $\gamma$  experiment [13] at the bottom of the negative-parity band.

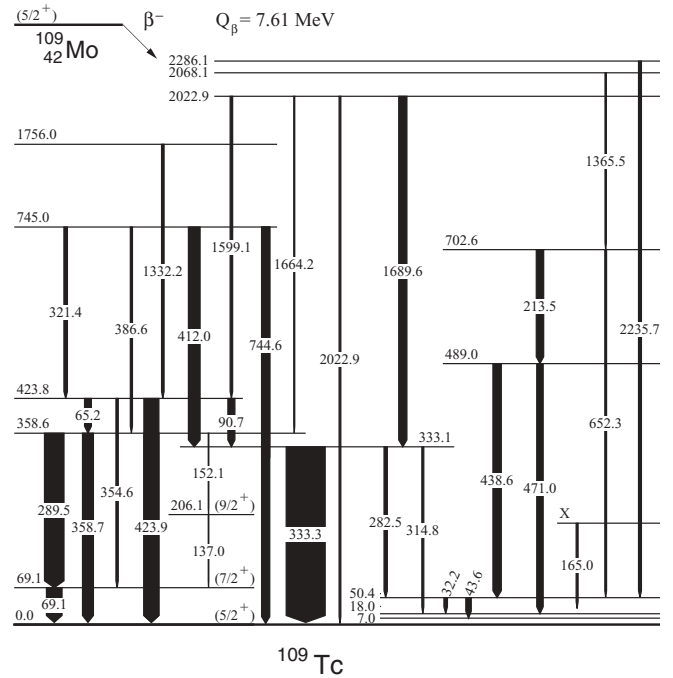


FIG. 5. Partial excitation scheme of  $^{109}\text{Tc}$  as obtained in the present work. The  $Q_\beta$  value was calculated based on the mass excess values measured with JYFLTRAP for  $^{109}\text{Mo}$  [22] and  $^{109}\text{Tc}$  [26].

A  $\gamma$  line of 128.7 keV was observed in the  $\beta^-$  decay of  $^{109}\text{Tc}$  [29]. In this work it is seen in both experiments with long and short collection tape cycles. In the second run the 128.7-keV peak is twice as intense as in the first run, when compared to the 194.6-keV line in  $^{109}\text{Ru}$  (see Table III). The significantly increased intensity when the collection tape was moved every second may indicate that the 128.7-keV line is fed by the  $\beta$  decay of  $^{109}\text{Mo}$  as well. According to Table III, one can estimate that about 51(9) intensity units of the 128.7-keV line belong to the  $^{109}\text{Mo}$  decay. As we did not see any additional coincidence with this line, it is not placed in the decay scheme.

### C. Experimental internal conversion coefficients

Using  $\gamma$  spectra measured by the LEPS detector we estimated the  $K_\alpha$  internal conversion coefficients (ICC) for low-energy  $\gamma$  lines in  $^{109}\text{Tc}$  by comparing their  $\gamma$  intensities to the intensity of the 18.3-keV  $K_\alpha$  x-ray line produced in their conversion process. In the case of the 69.1-keV line its total ICC was also found by the intensity balance in the 65.2–289.5–69.1-keV cascade. While gating on the 65.2-keV line the total intensities of the 69.1- and 289.5-keV transitions must be equal and thus the missing  $\gamma$  intensity of the 69.1-keV line is balanced by its total ICC. The experimental  $K$  shell, the total ICC, and the respective theoretical values are shown in Table IV.

### D. The estimate of the ground-state feeding

Table V presents an estimation of intensities of  $\beta$  decay to the ground states of isobars in the decay chain of  $^{109}\text{Mo}$ . In

TABLE I. Energies, relative intensities  $I_\gamma$ , and coincidence relations of  $\gamma$  lines observed in the  $\beta^-$  decay of  $^{109}\text{Mo}$ .

$E_\gamma$ (keV)	$I_\gamma$ (%)	Coincident $\gamma$ lines
$X-K_\alpha$		65.2, 69.1, 213.5, 289.5, 438.6
32.2(2)	11(3)	213.5, 438.6
43.6(2)	28.2(16)	213.5, (282.5), 438.6
65.2(2)	34.8(27)	18.3, 69.1, 289.5, 321.4, 358.7, (1599.1)
69.1(2) <sup>a,b</sup>	19–74	18.3, 65.2, (137.0), 289.5, 321.4, 354.6, 358.7, 386.6, (1332.2), (1664.2)
90.7(2)	36(5)	282.5, 314.8, 321.4, 333.3, (1332.2)
128.7(2) <sup>a,c</sup>	51(9)	
137.0(3) <sup>a</sup>	4(1)	(69.1), (152.1)
152.1(5)	1.4(3)	
165.0(3) <sup>c</sup>	4.1(4)	
213.5(2)	37.9(14)	18.3, 32.2, 43.6, 438.6, 471.0
282.5(2)	17.4(18)	18.3, 32.2, 43.6, 90.7, 412.1, 1689.6
289.5(2)	100(6)	18.3, 65.2, 69.1, 321.4, 386.6, (1599.1), 1664.2
314.8(3)	9.6(12)	90.7, 412.1
321.4(2)	17.9(9)	18.3, 65.2, 69.1, 90.7, 289.5, 333.3, (354.6), (358.7), 423.9
333.3(2)	200(9)	18.3, 90.7, 321.4, 412.1, 1689.6
354.6(4)	12.2(10)	18.3, 69.1, (321.4)
358.7(2) <sup>b</sup>	55.6(61)	18.3, 65.2, 69.1, 321.4, 386.6
386.6(3)	11.2(15)	18.3, 69.1, 289.5, 358.7
412.0(2)	60(9)	18.3, 282.5, (314.8), 333.3
423.9(2)	77.1(75)	321.4, 1332.2, 1599.1
438.6(2)	43.1(43)	18.3, 32.2, 43.6, 213.5, 1365.5
471.0(2)	33.3(34)	213.5, (1365.5)
652.3(3)	8.9(16)	18.3, (43.6)
744.6(2) <sup>b</sup>	41.7(49)	
1332.2(3)	20.2(17)	18.3, (65.2), (69.1), 90.7, (289.5), 333.3, 358.7, 423.9, 1174
1365.5(4)	6.6(8)	18.3, 438.6, 471.0
1599.1(3)	13.1(7)	(65.2), (69.1), (90.7), 289.5, 333.3, 423.9
1664.2(4)	5.2(6)	
1689.6(3)	41.5(25)	(282.5), 333.3
2022.9(3)	8.5(7)	
2235.7(3)	15.4(8)	(18.3), (32.2)

<sup>a</sup> Also in  $^{109}\text{Tc}$  decay.

<sup>b</sup> Also in  $^{109}\text{Ru}$  decay.

<sup>c</sup> Based on intensity ratio in two experiments.

the top row of Table V there are relative  $\beta$  decay intensities calculated with Bateman equations for the decay chain of  $^{109}\text{Mo}$ . The presented estimation was made for the case when a new monoisotopic source of  $^{109}\text{Mo}$  nuclei was delivered every  $t = 0.111$  s and the collection tape was moved after 2700 implantations, i.e., every  $T = 299.7$  s. To perform calculations for a series of decays in question two assumptions were made: (i) the first bunch of  $^{109}\text{Mo}$  nuclei after the collection tape movement is implanted into clean tape without any traces of radioactivity, and (ii) the nuclei in the decay chain of the  $^{109}\text{Mo}$  parent transform into its daughters only by the  $\beta^-$  process. For the  $\beta^-$ -decaying,  $A = 109$  isobars we used the

 TABLE II. Beta feedings and  $\log ft$  values of excited levels populated in the  $\beta^-$  decay of  $^{109}\text{Mo}$  and  $^{107}\text{Mo}$ . The data for the  $\log ft$  evaluation of the  $^{107}\text{Mo}$  decay are taken from Ref. [27].

$^{109}\text{Mo}$			$^{107}\text{Mo}$		
$E_{lev}$ (keV)	$I_\beta$ (%)	$\log ft$	$E_{lev}$ (keV)	$I_\beta$ (%)	$\log ft$
0.0	53(5)		0.0		>6.3
7.0		5.1	65.7		6.0
18.0			137.4		>6.8
50.4	9.3(14)	5.8	465.9	13.9	6.0
69.1	<3(1)	>6.3	495.8	8.8	6.2
206.1	0.14(6)	7.6	549.4	24.7	5.7
333.1	3.9(9)	6.1	850.6	50.8	5.3
358.6	3.4(7)	6.2	1374.7	8.3	5.9
423.8	9.6(1.3)	5.7			
489.0	2.1(4)	6.3			
702.6	2.2(3)	6.3			
745.0	7.3(1.1)	5.7			
1756.0	1.1(2)	6.2			
2022.9	4.0(5)	5.6			
2068.1	0.37(7)	6.6			
2286.1	0.9(1)	6.1			

following half-life values: 0.70 s (Mo) and 1.14 s (Tc) [30], 34.5 s (Ru) [31], and 80.0 s (Rh) [32].

For the first sample of the  $^{109}\text{Mo}$  parent nuclei the numbers of decays of Mo, Tc, Ru, and Rh were calculated over the whole time  $T$  till the next collection tape movement. For the second sample of parent nuclei implanted  $t$  seconds later, the numbers of decays were calculated over the remaining  $T - t$  period and added to the numbers of decays calculated for the first sample. In general, for the  $n$ th sample the numbers of decays of Mo, Tc, Ru, and Rh isobars were calculated over the remaining  $T - (n - 1)t$  seconds and added to the numbers of decays calculated for the previous  $n - 1$   $^{109}\text{Mo}$  samples. In this way the relative  $\beta^-$ -decay intensities in the decay chain of  $^{109}\text{Mo}$  were estimated as presented in the top row of Table V.

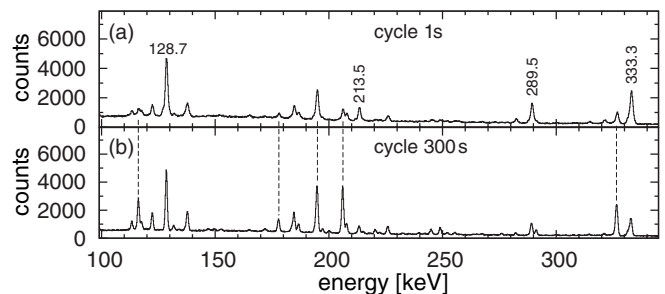


FIG. 6. Gamma spectra in the LEPS detector for  $^{109}\text{Mo}$  measured in two experiments. The collection tape was removing implanted ions every second (a) and every 300 s (b). The vertical lines mark the peaks 194.6 keV in the decay of  $^{109}\text{Tc}$  (0.86 s), 116.3 and 206.3 keV in the decay of  $^{109}\text{Ru}$  (34.5 s), and 178.0 and 326.8 keV in the decay of  $^{109}\text{Rh}$  (80 s). The peaks marked with energies are fed by  $\beta^-$  decay of  $^{109}\text{Mo}$ .

TABLE III. Intensity of the 128.7-keV line normalized to the intensity of the 194.6-keV line in  $^{109}\text{Ru}$ . The data come from a compilation [28] and the two experiments presented in this work.

$\gamma$ energy (keV)	$\gamma$ intensity		
	ENSDF	First expt.	Second expt.
128.7	51	59	124
194.6	100	100	100

One should note that these relative decay intensities depend only on the half-lives of the  $A = 109$  isobars and the interval  $T$  between consecutive collection tape movements.

For  $^{109}\text{Ru}$  and  $^{109}\text{Rh}$  there are compiled data on their  $\gamma$  intensities per 100  $\beta$  decays, including the ground-state feedings [28]. Thus it was possible to estimate experimentally the total number of  $\beta$  decays of Ru and Rh based on measured intensities of a few stronger  $\gamma$  lines populated by their  $\beta$  decays. Those experimental  $\beta$  intensities were compared to the calculated ones to find a relation (a normalization factor) between the measured and calculated  $\beta$  intensities. The final value of the normalization factor is an average from data for  $^{109}\text{Ru}$  and  $^{109}\text{Rh}$ . Certainly, the “quality” of such a normalization factor depends on the data on  $^{109}\text{Ru}$  and  $^{109}\text{Rh}$  found in the literature [28]. Experimental total  $\beta$  intensities for the decays of  $^{109}\text{Ru}$  and  $^{109}\text{Rh}$  calculated with the average normalization factor are given in the respective columns of the second row in Table V. As the data on Ru and Rh cover  $\beta$  feeding to excited and ground states the difference of their calculated and experimental  $\beta$  feedings, given in the respective columns in the third row of Table V, should equal zero—which is satisfied within error bars.

The calculation-to-experiment normalization factor was applied to the experimental  $\beta$  intensities for the decays of  $^{109}\text{Mo}$  and  $^{109}\text{Tc}$  to find  $\beta$  feedings to the excited states in Tc and Ru. The resulting values of 47(5) and 64(6) are shown in the respective columns of the second row in Table V. For

TABLE IV. Experimental and theoretical internal conversion coefficients for  $\gamma$  transitions fed by the  $^{109}\text{Mo}$   $\beta$  decay. Our experimental value for the 68.1-keV transition in  $^{109}\text{Rh}$  does not contradict with its known  $M1$  [29] character, which gives a check of the method.

$E_\gamma$ (keV)	K-shell conversion			Experiment (this work)	Proposed multipolarity
	Theory [33]				
	$E1$	$M1$	$E2$		
32.2	2.804	6.321	31.04		
43.6	1.234	2.627	14.56		
32.2 + 43.6				4.7(4)	
65.2	0.3357	0.8151	4.22	1.1(1)	$M1(+E2)$
69.1	0.3339	0.6874	3.474	0.9(2)	$M1(+E2)$
65.2 + 69.1				1.12(25)	
90.7	0.1541	0.3203	1.405	0.45(6)	$M1(+E2)$
68.1	0.3819	0.8890	3.772	1.5(3)	$M1$ [29]
	Total conversion				
69.1	0.382	0.788	4.68	0.90(20)	$M1$

TABLE V. Estimation of  $\beta$  feeding to the ground state in the decay of  $^{109}\text{Mo}$  and  $^{109}\text{Tc}$ . The relative simulated  $\beta$  decay intensity was estimated using Bateman equations for the decay chain of  $^{109}\text{Mo}$  monoisotopic samples.

$\beta$ -decaying nuclide	$^{109}\text{Mo}$	$^{109}\text{Tc}$	$^{109}\text{Ru}$	$^{109}\text{Rh}$
Simulated $\beta$ intensity	100	99.6	83.0	49.4
Expt. $\beta$ intensity	47(5)	64(6)	76(8)	49.6(20)
Unobserved $\beta$ intensity	53(5)	35(6)	7(8)	-0.2(20)

the  $\beta$  decays of  $^{109}\text{Mo}$  and  $^{109}\text{Tc}$  the difference between the calculated total  $\beta$  intensity and the experimental  $\beta$  intensity to the excited states is shown in the respective columns in the third row of Table V. The values of 35(6)% and 53(5)% can be interpreted as feedings to the ground state in the decay of  $^{109}\text{Tc}$  and to the ground and two low-lying states in the decay of  $^{109}\text{Mo}$  (see decay scheme in Fig. 5).

The uncertainties given in Table V were estimated based on statistical uncertainties of the  $\gamma$  intensities measured in this work and the uncertainties given in the compiled data on  $^{109}\text{Ru}$  and  $^{109}\text{Rh}$  [28].

### E. Spin of the ground state of $^{109}\text{Mo}$

The obtained multipolarity information on  $\gamma$  transitions in  $^{109}\text{Tc}$ , and, consequently, the information on spins of excited levels in  $^{109}\text{Tc}$ , is too limited for providing clear-cut information on the spin of the ground state of  $^{109}\text{Mo}$ . It is rather that one has to start with a certain assumption on the spin of the  $^{109}\text{Mo}$  nucleus to be able to interpret the excited levels in  $^{109}\text{Tc}$ .

In Ref. [34] spin and parity  $5/2^+$  have been proposed for the ground state of  $^{109}\text{Mo}$ . There it was mentioned that the  $3/2^+[411]$  neutron configuration, which forms the ground state in  $^{103}\text{Mo}$  and which is close to the  $5/2^+$  ground states in  $^{105}\text{Mo}$  and  $^{107}\text{Mo}$ , may also be close to the  $5/2^+$  ground state in  $^{109}\text{Mo}$ . The key question is whether this  $3/2^+$  configuration could be the ground state in  $^{109}\text{Mo}$ .

In  $^{107}\text{Mo}$  the  $3/2^+[411]$  band receives the population in the fission of  $^{248}\text{Cm}$ , which is comparable to the population of the  $5/2^+[413]$  ground-state band. It is then expected that if the  $3/2^+[411]$  configuration forms the ground state in  $^{109}\text{Mo}$  the population of the  $3/2^+[411]$  band in the fission of  $^{248}\text{Cm}$  should be at least as high as the population of the  $5/2^+$  ground-state band. This is not observed in the experiment. Furthermore, the  $3/2^+$  level, which is below the  $5/2^+$  level in  $^{105}\text{Mo}$ , raises above the  $5/2^+$  level in  $^{107}\text{Mo}$ . This is consistent with the Nilsson scheme for neutrons in this region of nuclei. Accordingly, in  $^{109}\text{Mo}$  the  $3/2^+[411]$  configuration is expected above the  $5/2^+[413]$  configuration.

We also note that the  $7/2^+$  and  $9/2^+$  levels, observed in  $^{109}\text{Tc}$  in prompt- $\gamma$  fission [13], are seen in the present data. The log  $ft$  values for these levels suggest even that both levels may be populated in  $\beta$  decay. This would exclude the  $3/2^+$  spin for the ground state in  $^{109}\text{Mo}$ . This optimistic scenario is weakened by the fact that there may be some unobserved feeding to the  $9/2^+$  level, which means that this level may be populated indirectly, via  $\gamma$  cascades, rather than directly

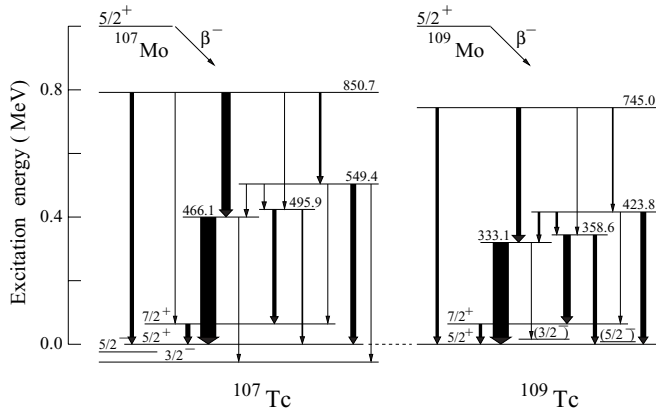


FIG. 7. Partial excitation schemes of  $^{107}\text{Tc}$  and  $^{109}\text{Tc}$ , populated in  $\beta^-$  decay of  $^{107}\text{Mo}$  and  $^{109}\text{Mo}$ , respectively. Levels are drawn relative to the  $5/2_1^+$  level, which is drawn at zero energy. The experimental energies of the levels are given in keV.

in  $\beta$  decay. One also has to note that the  $\log ft$  value limit  $>6.3$  (see Table II) for the 69.1-keV level is too high for  $\beta$  decay from a  $5/2^+$  level to a  $7/2^+$  level, unless there is some unknown hindrance.

It is instructive to compare  $\beta$  decay schemes of  $^{109}\text{Mo}$  and  $^{107}\text{Mo}$ . We note that, with high confidence, the spin of the ground state of  $^{107}\text{Mo}$  is  $5/2^+$  [35]. From the available  $\gamma$  intensities in  $^{107}\text{Tc}$  [27] we have evaluated  $\log ft$  values for levels in  $^{107}\text{Tc}$ , which are shown in Table II. In Fig. 7 we display fragments of  $\beta$  decay schemes for  $^{107}\text{Mo}$  [27] and for  $^{109}\text{Mo}$ . There are obvious similarities between the two decay schemes, which further support a spin  $5/2^+$  assignment for the ground state of  $^{109}\text{Mo}$ . Therefore we conclude that spin  $5/2^+$  for the ground state in  $^{109}\text{Mo}$  is at present the most likely solution, and this will be adopted in further discussions in this work.

#### F. Spin and parity assignments to levels in $^{109}\text{Tc}$

We assign spins and parity  $7/2^+$  and  $9/2^+$  to the 69.1- and the 206.1-keV levels, respectively, assuming that these levels are the same as the two lowest excited states in the  $5/2^+$  band, observed in prompt- $\gamma$  fission [13], because they show the same energies and decays.

There are three low-lying excited levels at 7.0, 18.0, and 50.4 keV which are candidates for the low-spin excitations in  $^{109}\text{Tc}$  suggested in Fig. 1. The combined  $K$ -conversion coefficient for the 32.2- and 43.6-keV transitions,  $\alpha_K = 4.7(4)$ , indicates that at least one of these transitions should have an  $E1$  multipolarity. Therefore, the three discussed levels can not all have the same parity. The experimental  $\alpha_K$  value is in between the theoretical solutions (i)  $\alpha_K^{th} = 4.04$  obtained when both transitions are  $E1$  and (ii)  $\alpha_K^{th} = 5.43$  obtained when the 32.2-keV transition is an  $E1$  and the 43.6-keV transition has pure  $M1$  multipolarity (with other solutions being further away from the experimental value). Furthermore, one expects two of the three levels to have negative parity, according to Fig. 1. This leaves three solutions, (a), (b), and (c), which are sketched in Fig. 8.

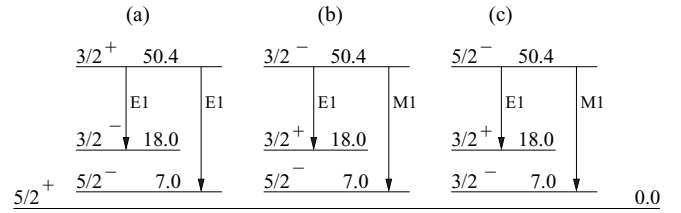


FIG. 8. Spin and parity hypothesis available for the low-energy excitation in  $^{109}\text{Tc}$ . See text for further discussion.

In  $^{107}\text{Tc}$  one observes an  $E1$  link between the  $5/2^+$  bandhead at 65.6 keV and the  $5/2^-$  bandhead at 45.6 keV [27]. It is likely that such a link should be also present in  $^{109}\text{Tc}$ . In Ref. [13] an upper limit on the energy of this link has been put at 30 keV. Therefore, we reject solution (c). Consequently, the  $5/2^-$  state should be assigned to the 7.0-keV level. Furthermore, in  $^{107}\text{Tc}$  there is a strong  $E1$  link between the  $5/2^+$  bandhead and the  $3/2^-$  ground state, which is also expected in  $^{109}\text{Tc}$ . The absence of this link in  $^{109}\text{Tc}$  makes solution (b) less likely. The remaining solution, (a), with two  $E1$  transitions, fits well the Alaga rules for the  $E1$  transitions but it has to be mentioned that the nonobservation of the 50.4-keV transition remains unexplained. Therefore the proposed spin and parity assignments are tentative.

In this work we observe, in singles spectra, a line at 165.0 keV. It is possible that this line corresponds to the 165.0-keV transition of the ( $5/2^-$ ) band reported in the prompt- $\gamma$  work [13]. Thus we tentatively propose spin  $7/2^-$  for the level assigned as  $X$ , shown in Fig. 5.

By considering the observed branchings and the  $\log ft$  value for the 333.1-keV level, the most likely spin and parity assignment for this level is  $3/2^+$ . A similar conclusion can be drawn for the analogous 466.1-keV level in  $^{107}\text{Tc}$ , shown in Fig. 7.

The  $M1 + E2$  multipolarity and high intensity of the 65.2- and 90.7-keV transitions indicate that the 333.1-, 358.6- and 423.8-keV levels have the same parity and similar structure. Therefore the absence of the transition between the 358.6- and 333.1-keV levels suggests a spin difference  $\Delta I > 1$  between these two levels and, thus, spin  $7/2^+$  for the 358.6-keV level. Consequently, the 423.8-keV level should have spin and parity  $5/2^+$ . These assignments are consistent with the observed branchings and  $\log ft$  values for the 358.6- and 423.8-keV levels. Analogous spin and parity assignments can be made for the 495.9- and 549.4-keV levels in  $^{107}\text{Tc}$ , shown in Fig. 7.

#### IV. DISCUSSION

The  $5/2^+$  ground state in  $^{109}\text{Mo}$  is dominated by the mixed  $5/2^+$  [402] and  $5/2^+$  [413] neutron configurations [34], originating from the  $\nu g_{7/2}$  and  $\nu d_{5/2}$  orbitals, while the ground state of  $^{109}\text{Tc}$  is dominated by the  $5/2^+$  [422] proton configuration originating from the  $\pi 1g_{9/2}$  orbital. The similarity of the initial and the final wave functions is consistent with the strong feeding of the  $5/2^+$  ground state of  $^{109}\text{Tc}$  in the  $\beta$  decay of  $^{109}\text{Mo}$ , which does not require a change of spin, angular momentum, or parity. We note that the  $5/2^+$  [402]

single-particle configurations have been also proposed for the ground states in  $^{107}\text{Mo}$  and  $^{111}\text{Ru}$  neighbors of  $^{109}\text{Mo}$  [36].

The  $5/2^-$  and  $3/2^-$  spin and parity assignments proposed in this work for the 7.0- and 18.0-keV levels are consistent with the  $5/2^-$ [303] and  $3/2^-$ [301] proton configurations originating from the  $\pi f_{5/2}$  and  $\pi p_{3/2}$  orbitals. It is expected that the  $\beta$  feeding to these two levels should be smaller than the feeding to the ground state because it requires both a change of angular momentum and parity. In this work we could not single out the  $\beta$  feeding to the 7.0- and 18.0-keV levels but it is likely that the large feeding indicated in Table II for the group of the three levels—the ground state and those at 7.0 and 18.0 keV—goes mostly to the ground state. Excitation energies of the  $\pi 3/2^-$ [301] and  $\pi 5/2^-$ [303] configurations, calculated in Ref. [13] using the quasiparticle-rotor model (QPRM) [37–40], fit well the known  $3/2^-$  and  $5/2^-$  levels in  $^{107}\text{Tc}$  [27] and the  $3/2^-$  and  $5/2^-$  levels in  $^{109}\text{Tc}$ , which are newly proposed in this work.

The assignment of spin and parity  $3/2^+$  to the 50.4-keV level makes it a good candidate for a member of the  $1/2^+$ [431] intruder band, originating from the  $\pi 2d_{5/2}$  orbital. The strong  $\beta$  decay to the 50.4-keV level could be explained by the similarity of the corresponding wave functions, both of which contain a contribution from the  $\pi 2d_{5/2}$  orbital. The  $1/2^+$ [431] intruder configuration in  $^{107}\text{Tc}$  has been well reproduced by the QPRM calculations in Ref. [41]. It has been found there that this configuration has a large prolate deformation and is also triaxial. The deformation parameter,  $\epsilon_2 = 0.35$ , used to reproduce the intruder band is higher than that used for the ground state ( $\epsilon_2 = 0.33$ ) but the triaxial deformation of the intruder,  $\gamma = 19^\circ$ , has been found to be smaller than the triaxial deformation of the ground state ( $\gamma = 23^\circ$ ). In  $^{109}\text{Tc}$  we were able to reproduce the 50-keV excitation energy proposed for the  $3/2^+$  member of the  $1/2^+$ [431] intruder with very similar parameters of  $\epsilon_2 = 0.35$  and  $\gamma = 20^\circ$ . This consistency supports the proposed interpretation of the 50.4-keV level in  $^{109}\text{Tc}$ .

In Fig. 9 we show the near-yrast, positive-parity excitations in Tc isotopes (relative to the position of the  $9/2_1^+$  level). There are three groups of levels. The yrast levels (open circles) correspond to the  $K = 5/2$  rotational band build on top of the

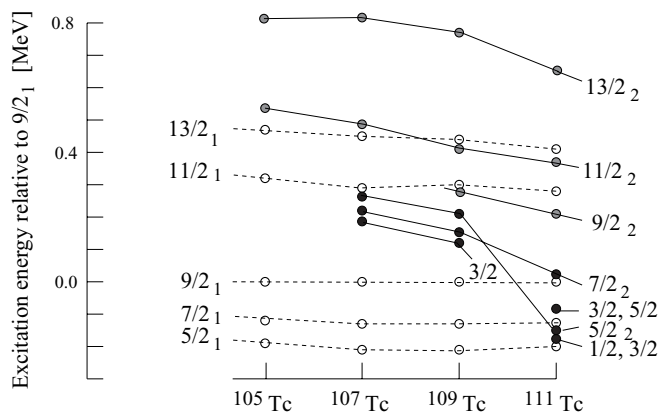


FIG. 9. Systematic behavior of selected low-energy excitations in Tc isotopes. See text for further explanation.

$5/2^+$ [422] proton configuration in a prolate potential. This ground-state solution in the Tc isotopes shown does not vary much with increasing number of neutrons, though there is some increase in deformation from  $^{105}\text{Tc}$  to  $^{111}\text{Tc}$ .

The second group (gray circles) comprises levels which were classified as  $K = 9/2$  members of a triaxial band in a prolate potential, built on top of the ground-state configuration [13] (and the 425.0-keV level in  $^{111}\text{Tc}$  may be the  $9/2_2^+$  excitation as well [7]). As can be seen in the figure, triaxiality increases with increasing neutron number, which is reflected by the lowering of excitation energies of levels in this group, when the number of neutrons increases.

Levels belonging to the third group (black circles in Fig. 9) show in  $^{107}\text{Tc}$  and  $^{109}\text{Tc}$  a trend similar to that of the levels from the  $K = 9/2$  band. Interestingly, no decay of the  $9/2_2^+$  level with  $K = 9/2$  to the  $7/2_2^+$  level has been observed in  $^{107}\text{Tc}$ ,  $^{109}\text{Tc}$ , or  $^{111}\text{Tc}$ , despite the expected similar origin of these levels. For example, in  $^{109}\text{Tc}$  such a link would correspond to a  $M1 + E2$  transition of 130 keV, a decay which should be fast. Its nonobservation suggests a strong hindrance.

The three levels at 333.1, 358.6, and 423.8 keV in  $^{109}\text{Tc}$ , belonging to the third group, for which we have proposed spins and parities of  $3/2^+$ ,  $7/2^+$ , and  $5/2^+$ , respectively, represent a new type of excitation, not observed in prompt- $\gamma$  fission [13], probably because of their nonyrast nature. These levels can be interpreted as  $K = 1/2$  members of the triaxial band built on top of the ground-state configuration,  $\pi 5/2^+$ [422]. In Fig. 10 we show the QPRM calculations in a prolate potential for  $^{107}\text{Tc}$ ,  $^{109}\text{Tc}$ , and  $^{111}\text{Tc}$ . (These results were not shown in Ref. [13] due to the lack of the corresponding experimental data.) To help the comparison we show the corresponding experimental energies in the discussed Tc isotopes (with two  $3/2^+$  candidates being shown for  $^{111}\text{Tc}$ ). The reproduction of the  $3/2^+$ ,  $5/2^+$ , and  $7/2^+$  triplet in  $^{107}\text{Tc}$  and  $^{109}\text{Tc}$  is good. We note that, with this interpretation, the very large difference in the  $K$  number between the  $7/2_2^+$  and  $9/2_2^+$  levels could cause the hindrance of the transition linking these two levels, even if

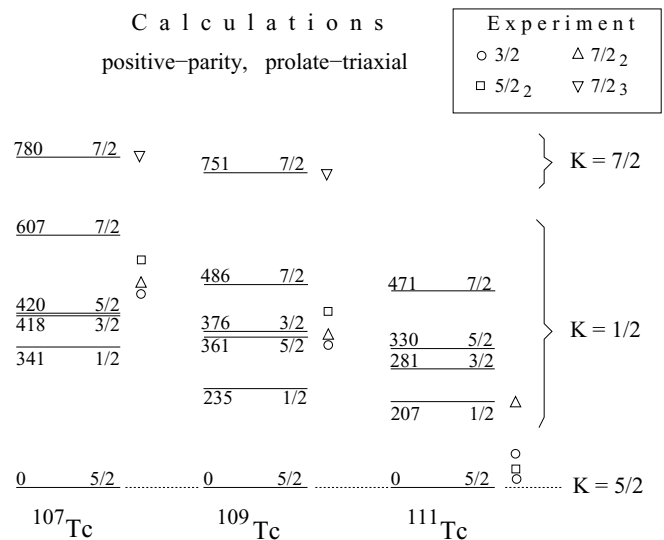


FIG. 10. QPRM results for positive-parity levels in a prolate potential in Tc isotopes.

the corresponding  $K$  numbers are not pure, which is the case in a nucleus with a triaxial deformation or  $\gamma$  softness.

The reproduction of the experiment with the prolate solutions is much worse in  $^{111}\text{Tc}$ , as already noted in Ref. [7]. The sudden drop of the  $5/2_2^+$  excitation energy, seen in Fig. 9, supports the transition from prolate to oblate deformation, as proposed in Ref. [7]. It is interesting to note that the  $5/2_2^+$  calculated at 10 keV in  $^{111}\text{Tc}$  in Ref. [7] is the same  $\pi$   $5/2^+[422]$  configuration with  $K = 1/2$  but calculated in an oblate potential. However, while there is no decay from the  $9/2_2^+$  to the  $7/2_2^+$  level, which agrees with the hypothesis of a large difference in the  $K$  number, the decay from the  $9/2_2^+$  to the  $5/2_2^+$  level at 42.6 keV is seen [7]. This may raise further questions about the structure of the  $5/2_2^+$  level. It is possible that the  $5/2_2^+$  level results from mixing of the prolate and oblate solutions, as suggested in more advanced calculations [8,9]. Such a mixing could alter the picture obtained with our simple QPRM calculations. Clearly, more theoretical effort is needed to produce details of such mixed configurations and their decays.

In Fig. 7 there are characteristic levels in  $^{107}\text{Tc}$  and  $^{109}\text{Tc}$  at 850.7 and 745.0 keV, respectively, which have very similar decays in both nuclei and are clearly linked with the  $3/2_2^+$ ,  $5/2_2^+$ , and  $7/2_2^+$  triplet of levels. These levels cannot correspond to the  $K = 1/2$  configuration with spin  $1/2^+$  or  $9/2^+$ , given the observed branchings. We also note that they decay as well to the  $K = 5/2$  ground state. The closest QPRM solution is the  $7/2^+[413]$  configuration with  $K = 7/2$ , originating from the  $\pi$   $g_{9/2}$  orbital. This is the third-lowest single-particle configuration of positive parity in the discussed Tc isotopes, after the  $5/2^+[422]$  ground state and the  $1/2^+[431]$  intruder.

In Ref. [13] the  $7/2^+$  level with  $K = 7/2$  in  $^{109}\text{Tc}$  has been calculated at 634 keV, somewhat below the experimental counterpart, proposed at 745.0 keV. We have already noticed that various configurations in a given nucleus may correspond to slightly different deformations. For example, there are consistent differences between deformations of the  $5/2^+[422]$  ground-state configuration and the  $1/2^+[431]$  intruder in  $^{107}\text{Tc}$  and  $^{109}\text{Tc}$ . In Ref. [13] we also indicated different deformation (both quadrupole deformation and triaxiality) for the negative-parity configuration. Therefore, the  $7/2^+[413]$  configuration may correspond to a slightly different deformation. We have found that with a quadrupole deformation parameter  $\epsilon_2 = 0.30$  and triaxiality parameter  $\gamma = 19^\circ$ , we could reproduce well the discussed levels in both nuclei, as shown in Fig. 10. This supports the proposed spin and configuration assignment to the 850.7-keV level in  $^{107}\text{Tc}$  and the 745.0-keV level in  $^{109}\text{Tc}$ .

An intriguing remaining question concerns the  $1/2^+$  level shown in Fig. 10, which is predicted in  $^{107}\text{Tc}$ ,  $^{109}\text{Tc}$ , and  $^{111}\text{Tc}$  at rather low energy but not observed experimentally (but in  $^{111}\text{Tc}$  this could be one of the levels around 200 keV

without spin assignment [7]). It is likely that such a collective excitation with  $K = 1/2^+$  is not populated in the  $\beta$  decay of a  $K = 5/2$  single-particle configuration. However, in  $^{109}\text{Tc}$  one would expect a decay from the  $K = 1/2$ ,  $I^\pi = 3/2^+$  level to this  $K = 1/2$ ,  $I^\pi = 1/2^+$  level, considering the predicted transition energy of 141 keV, which was not observed in the experiment.

## V. SUMMARY

We have studied nonyrast levels in  $^{109}\text{Tc}$ , which could not be observed in the previous, prompt- $\gamma$  works. The levels were populated in the  $\beta^-$  decay of  $^{109}\text{Mo}$  nuclei, produced in the fission of natural uranium induced by 25-MeV deuterons and separated by IGISOL3 and the JYFLTRAP facilities of the University of Jyväskylä. In  $^{109}\text{Tc}$  we have found 13 new levels for which spins and parities have been proposed. The spin and parity assignment  $5/2^+$  for the ground state of  $^{109}\text{Mo}$ , proposed in a prompt- $\gamma$  study, is confirmed in the present work. Three low-energy excitations are interpreted as single-particle, proton configurations  $3/2^- [301]$ ,  $5/2^- [303]$ , and  $1/2^+ [431]$ , which were expected here based on systematic predictions. These configurations are well reproduced by the quasiparticle-rotor model. We have also found three excitations, which we interpret as members of the  $K = 1/2$  triaxial band built on top of the  $5/2^+[422]$  ground-state configuration. Similar excitations are proposed in  $^{107}\text{Tc}$ , for which  $\beta^-$  decay has been studied in another work. Excitation schemes of both nuclei are very similar but differ clearly from the scheme of  $^{111}\text{Tc}$ . This breakdown of the systematics is interpreted as a transition from prolate to oblate deformation. There is a clear need for further studies of  $^{107}\text{Tc}$ ,  $^{109}\text{Tc}$ , and  $^{111}\text{Tc}$ , both experimental and theoretical. Especially important would be firm spin and parity assignments in all three Tc isotopes (in particular one should determine multipolarities of the 32.2- and 43.6-keV transitions in  $^{109}\text{Tc}$ ) and the search for the  $K = 1/2$ ,  $I^\pi = 1/2^+$  levels in  $^{107}\text{Tc}$  and  $^{109}\text{Tc}$ , predicted by the calculation at rather low energies. The experimental information on triaxiality in neutron-rich Mo, Tc, and Ru isotopes is one of the richest data sets available for testing nuclear models.

## ACKNOWLEDGMENTS

This work has been supported by the Polish MNiSW Grant No. N N202 007334, the EU 6th Framework programme “Integrating Infrastructure Initiative—Transnational Access,” Contract No 506065 (EURONS), and the Academy of Finland under Project No. 111428 and the Finnish Center of Excellence Programme 2006–2011 (Nuclear and Accelerator Based Physics Programme at JYFL). We also want to thank Dr. S. Rahaman and Dr. P. Karvonen for their help during the experiment.

- [1] P. Möller, R. Bengtsson, B. Gillis Carlsson, P. Olivius, and T. Ichikawa, *Phys. Rev. Lett.* **97**, 162502 (2006).  
 [2] A. Guessous *et al.*, *Phys. Rev. Lett.* **75**, 2280 (1995).

- [3] J. A. Shannon *et al.*, *Phys. Lett. B* **336**, 136 (1994).  
 [4] F. R. Xu, P. M. Walker, and R. Wyss, *Phys. Rev. C* **65**, 021303 (2002).

- [5] W. Urban, T. Rzača-Urban, J. L. Durell, W. R. Phillips, A. G. Smith, B. J. Varley, I. Ahmad, and N. Schulz, *Eur. Phys. J. A* **20**, 381 (2004).
- [6] W. Urban, T. Rzača-Urban, J. L. Durell, A. G. Smith, and I. Ahmad, *Eur. Phys. J. A* **24**, 161 (2005).
- [7] J. Kurpeta *et al.*, *Phys. Rev. C* **84**, 044304 (2011).
- [8] P. Sarriguren and J. Pereira, *Phys. Rev. C* **81**, 064314 (2010).
- [9] R. Rodríguez-Guzmán, P. Sarriguren, L. M. Robledo, and S. Perez-Martin, *Phys. Lett. B* **691**, 202 (2010).
- [10] W. Urban, T. Rzača-Urban, J. L. Durell, A. G. Smith, and I. Ahmad, *Phys. Rev. C* **70**, 057308 (2004).
- [11] A. Bauchet *et al.*, *Eur. Phys. J. A* **10**, 145 (2001).
- [12] Y. X. Luo *et al.*, *Phys. Rev. C* **70**, 044310 (2004).
- [13] W. Urban, J. A. Pinston, T. Rzača-Urban, J. Kurpeta, A. G. Smith, and I. Ahmad, *Phys. Rev. C* **82**, 064308 (2010).
- [14] Y. X. Luo *et al.*, *Phys. Rev. C* **74**, 024308 (2006).
- [15] L. Gu *et al.*, *Phys. Rev. C* **79**, 054317 (2009).
- [16] L. Gu *et al.*, *Chin. Phys. Lett.* **26**, 092502 (2009).
- [17] J. Äystö, *Nucl. Phys. A* **693**, 477 (2001).
- [18] H. Penttilä *et al.*, *Eur. Phys. J. A* **25**, 745 (2005).
- [19] A. Nieminen, J. Huikari, A. Jokinen, J. Äystö, P. Campbell, E. C. A. Cochrane (EXOTRAPs Collaboration), *Nucl. Instrum. Methods Phys. Res. A* **469**, 244 (2001).
- [20] T. Eronen and J. C. Hardy, *Eur. Phys. J. A* **48**, 46 (2012).
- [21] S. Rinta-Antila *et al.*, *Eur. Phys. J. A* **31**, 1 (2007).
- [22] U. Hager *et al.*, *Phys. Rev. Lett.* **96**, 042504 (2006).
- [23] G. Savard, St. Becker, G. Bollen, H.-J. Kluge, R. B. Moore, Th. Otto, L. Schweikhard, H. Stolzenberg, and U. Wiess, *Phys. Lett. A* **158**, 247 (1991).
- [24] J. Äystö *et al.*, *Phys. Rev. Lett.* **69**, 1167 (1992).
- [25] H. Penttilä, K. Eskola, P. Jauho, A. Jokinen, M. E. Leino, P. Taskinen, J. Äystö, Annual Report 1989–1990, University of Jyväskylä 77, 1990 (unpublished).
- [26] U. Hager *et al.*, *Phys. Rev. C* **75**, 064302 (2007).
- [27] J. Blachot, *Nuclear Data Sheets* **109**, 1383 (2008).
- [28] Evaluated Nuclear Structure Data File, [www.nndc.bnl.gov](http://www.nndc.bnl.gov).
- [29] H. Penttilä, Ph.D. thesis, University of Jyväskylä, 1992.
- [30] J. Pereira *et al.*, *Phys. Rev. C* **79**, 035806 (2009).
- [31] N. Kaffrell *et al.*, *Nucl. Phys. A* **470**, 141 (1987).
- [32] M. Kanazawa, S. Ohya, T. Tamura, Z.-I. Matumoto, and N. Mutsuro, *J. Phys. Soc. Jpn.* **44**, 25 (1978).
- [33] T. Kibédi, T. W. Burrows, M. B. Trzhaskovskaya, P. M. Davidson, C. W. Nestor, Jr., *Nucl. Instrum. Methods Phys. Res. A* **589**, 202 (2008).
- [34] W. Urban, Ch. Droste, T. Rzača-Urban, A. Złomaniec, J. L. Durell, A. G. Smith, B. J. Varley, and I. Ahmad, *Phys. Rev. C* **73**, 037302 (2006).
- [35] W. Urban, T. Rzača-Urban, J. A. Pinston, J. L. Durell, W. R. Phillips, A. G. Smith, B. J. Varley, I. Ahmad, and N. Schulz, *Phys. Rev. C* **72**, 027302 (2005).
- [36] C. Goodin *et al.*, *Phys. Rev. C* **80**, 014318 (2009).
- [37] S. E. Larsson, G. Leander, and I. Ragnarsson, *Nucl. Phys. A* **307**, 189 (1978).
- [38] T. Bengtsson and I. Ragnarsson, *Nucl. Phys. A* **436**, 14 (1985).
- [39] P. Semmes and I. Ragnarsson (private communication).
- [40] J. A. Pinston, W. Urban, Ch. Droste, T. Rzača-Urban, J. Genevey, G. S. Simpson, J. L. Durell, A. G. Smith, B. J. Varley, and I. Ahmad, *Phys. Rev. C* **74**, 064304 (2006).
- [41] G. Simpson, J. Genevey, J. A. Pinston, U. Köster, R. Orlandi, A. Scherillo, and I. A. Tsekhanovich, *Phys. Rev. C* **75**, 027301 (2007).